Turkish Journal of Electrical Engineering and Computer Sciences

Volume 30 | Number 4 Article 4

5-1-2022

Dual-polarized elliptic-H slot-coupled patch antenna for 5G applications

EMRE ALP MİRAN

MEHMET ÇİYDEM

Follow this and additional works at: https://journals.tubitak.gov.tr/elektrik

 Part of the Computer Engineering Commons, Computer Sciences Commons, and the Electrical and Computer Engineering Commons

Recommended Citation

MİRAN, EMRE ALP and ÇİYDEM, MEHMET (2022) "Dual-polarized elliptic-H slot-coupled patch antenna for 5G applications," *Turkish Journal of Electrical Engineering and Computer Sciences*: Vol. 30: No. 4, Article 4. https://doi.org/10.55730/1300-0632.3844
Available at: https://journals.tubitak.gov.tr/elektrik/vol30/iss4/4

This Article is brought to you for free and open access by TÜBİTAK Academic Journals. It has been accepted for inclusion in Turkish Journal of Electrical Engineering and Computer Sciences by an authorized editor of TÜBİTAK Academic Journals. For more information, please contact academic.publications@tubitak.gov.tr.

Turkish Journal of Electrical Engineering & Computer Sciences

http://journals.tubitak.gov.tr/elektrik/

Research Article

Turk J Elec Eng & Comp Sci
(2022) 30: 1204 – 1218
© TÜBİTAK
doi:10.55730/1300-0632.3844

Dual-polarized elliptic-H slot-coupled patch antenna for 5G applications

Emre A. MİRAN[1,*], **Mehmet ÇİYDEM**[2]

[1]Department of Electrical and Electronics Engineering, Faculty of Engineering, Middle East Technical University, Ankara, Turkey

[2]Department of Electrical and Electronics Engineering, Faculty of Engineering, Gazi University, Ankara, Turkey

Received: 05.05.2021 • **Accepted/Published Online:** 03.09.2021 • **Final Version:** 31.05.2022

Abstract: A dual-polarized, slot-coupled dielectric patch antenna design is presented in sub-6 GHz for 5G base stations. Proposed antenna is implemented using two dielectric patch layers (main patch and parasitic patch) above a feeding line layer. Excitation is realized by crossed elliptic-H slots in order to create orthogonal $\pm 45^\circ$ polarizations. Through the use of patches at proper heights together with elliptic-H slots, significant improvement in impedance bandwidth, matching level, isolation and front-to-back ratio is acquired. Prototype antenna has an impedance bandwidth of 18.5% (3.23–3.85 GHz) for $|S_{11}|$, $|S_{22}| < -15$ dB, covering the 5G spectra of 3.30–3.80 GHz. The isolation between ports ($|S_{21}|$) is obtained as < -25 dB in desired operating band. Antenna exhibits stable, broadside radiation patterns with half power beam-widths of 59°–64° and 69°–72° in E/H-planes, respectively. Gain of the antenna varies within the range of 7.9–8.4 dBi. Proposed antenna is also low profile (9.8 mm). It needs no reflector or cavity-backed structure and meets all the requirements of 5G base stations as an antenna element. Design details, numerical studies, and experimental results are presented.

Key words: Dual-polarization, slot coupling, isolation, low profile, broadband patch antenna, sub-6 GHz, 5G, base station antenna

1. Introduction

Along with the development of cellular communication in the last decade, continuous increase in number of users has led to demanding requirements for base station antennas such as low profile, wide operational bandwidth (BW), good impedance matching ($|S_{11}|$, $|S_{22}| < -15$ dB), high channel isolation ($|S_{21}| < -20$ dB), high front-to-back ratio (FBR > 20 dB) and high cross-polar discrimination level (XPD > 20 dB). Dual-polarization is also employed in base stations antennas for diversity against multipath fading [1–3]. Furthermore, it enables the use of two well-isolated channels at both transmitting and receiving sides on the same physical antenna structure in a compact manner.

The literature has focused on different types of designs for dual-polarized antennas in sub-6 GHz region. Classical crossed-dipole antennas, which are composed of a pair of dipoles in 45° orientation, are most widely used since they can provide wide impedance BW and strong isolation [3, 4]. They also have high FBR since there is almost no backward radiation. However, they have generally high profile and bulky feeding structure with balun. Several crossed-dipole structures for 5G are designed in [5–7]. Although magneto-electric dipoles in [8–10], which can also be regarded as crossed-dipole antenna, are low profile, they have complex feeding and

*Correspondence: elektrik@tubitak.gov.tr

This work is licensed under a Creative Commons Attribution 4.0 International License.

radiating structure.

Patch antennas are also widely used for dual-polarization due to their compactness, low profile, and ease of manufacturing [1]. Despite their narrow band nature in early time, different feeding techniques have been developed to extend their operating bandwidth. Probe feeding and slot coupling are common types for exciting the patches. Together with such feedings, multilayer stacked patches can also be employed for broadband operation. Several variations of probe feeding (meandering, and hook shapes, symmetric or antisymmetric feeds, etc.) for dual-polarized patch antennas are given in [11–16]. Other common type of feeding for dual-polarized patch antennas is slot coupling, again in single or multilayer configuration. Dual-polarization feature of antenna is implemented by either crossed slots centered on common ground or two separate slots in orthogonal placement [18**?** –23]. The crossed-slot configuration is more common because of its single layer feeding, making the antenna low profile and compact. In [17], a dual-polarized stacked patch antenna is designed by utilizing a plus-like shaped slot. A four layer microstrip patch antenna is presented in [18] where the feeding lines for each polarization are mounted on separate layers and slots are etched on these layers accordingly. In [19], two modified-H slots are used to excite dual-polarization on the patch. [21, 22] report square shaped ring slot structure feeding a patch and Jerusalem crossed radiator, respectively. In [23], a broadband multilayer patch antenna containing a quasi-crossed-shaped slot is presented. Additional different designs of slot coupled patch antennas can be found in [24–26].

In this paper, design of a simple, broadband, dual-polarized, slot-coupled patch antenna with low profile and easy fabrication is presented for 5G base stations to operate in 3.30–3.80 GHz band. Prototyped antenna exhibits 18.5% (3.23–3.85 GHz) impedance BW for $|S_{11}|$, $|S_{22}| < -15$ dB, isolation $|S_{21}| < -25$ dB, FBR > 23 dB and XPD > 22 dB with a gain of 7.9–8.4 dBi. Broadside, directional radiation patterns have been obtained with half power beamwidths (HPBWs) of 59°–64° in E-plane and 69°–72° in H-plane. In addition to these performances, other outstanding feature of antenna can be counted as its simplicity and low-profile. It must be noted that slot-coupled patch antennas may be simple, low profile, however, their FBR performance is poor because of undesirable back radiation of the slots. Hence reflector plane or cavity backed structure, which increases antenna profile, is generally employed to make FBR higher. Proposed antenna has low-profile (9.8 mm) and good FBR with no reflector.

2. Antenna design

2.1. Geometry and configuration

The antenna comprises two dielectric patch layers (main and parasitic one) and a feedline layer, all separated by air. Height of the main patch layer is denoted by hm1 whereas separation between the patch layers is denoted by hm2. Patches are square-shaped whose lenghts are Lm1 and Lm2. The feedline layer consists of a feeding network of the antenna at its bottom side and a common ground at its upper side. Elliptic-H slots are etched on this ground side. Feeding network is composed of two parts: matching section and 100 Ω branch lines. Matching section provides broadband matching between input impedance of patches and 50 Ω SMA port. It includes a two-section binomial transformer and an additional rectangular stub of size $3.1 \times 4.0\ mm^2$. Sections of the transformer are approximately quarter wavelength (Lt1, Lt2) at center frequency, $f_c = 3.55$ GHz ($\lambda_c = 84.5$ mm). Coupling to the slots is realized using two 100 Ω microstrip branch lines which are connected to the matching section through a T-junction. Branch lines are separated by a distance Ld and terminated by L-shaped stubs in order to compensate the reactive component of the input impedance of the patches and

preclude the overlap. Due to the inevitable crossing between inner branches, a small air bridge is introduced here to avoid intersection. All dielectric layer are implemented by using FR4 substrate ($\varepsilon_r = 4.4$, $tan\delta = 0.02$) of height 1.6 mm. Geometry of the antenna is illustrated in Figure 1 while physical dimensions are given in Table 1.

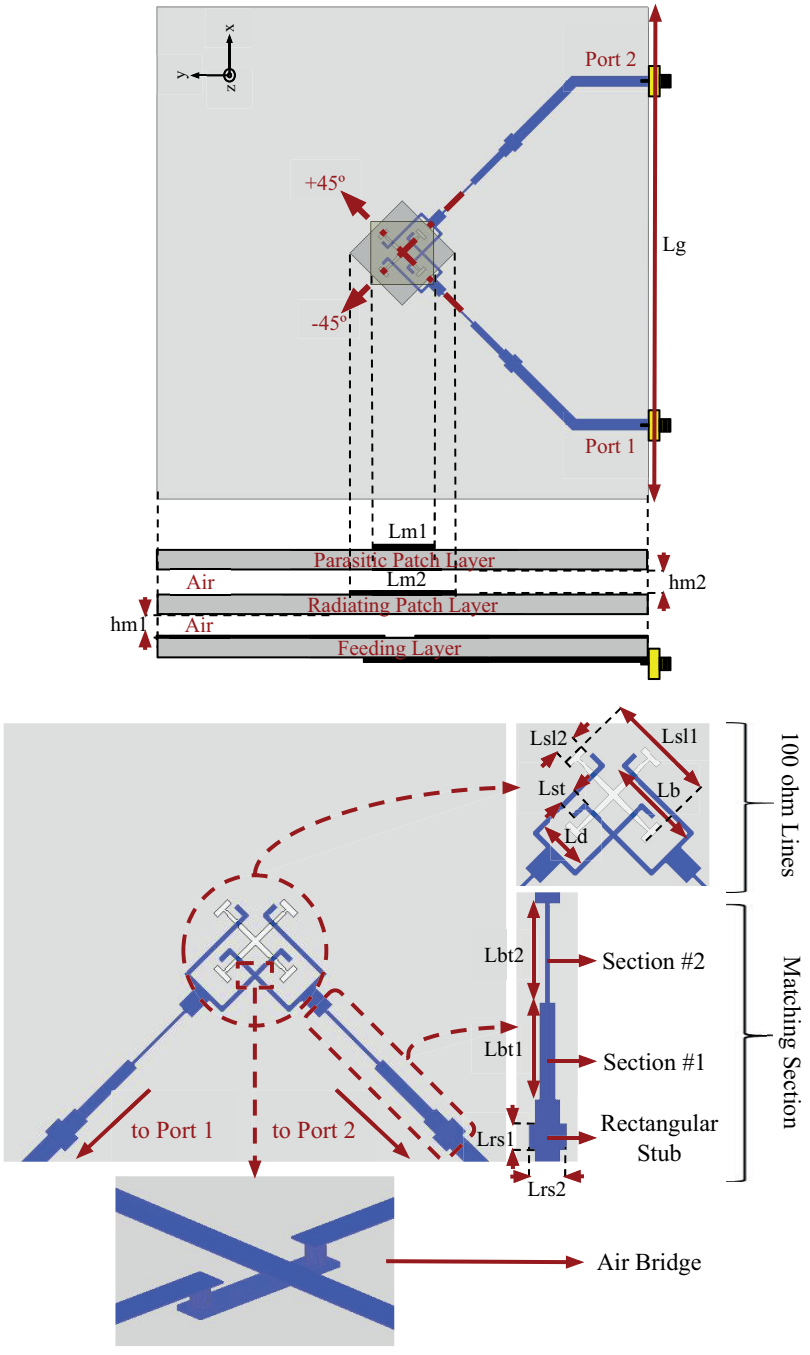


Figure 1. Antenna geometry and configuration a) top view and cross-sectional view, b) elliptic-H slots, feedlines and binomial transformer.

Table 1. Dimensions of the proposed antenna.

Description	**Parameter**	**Dimension [mm]**
Ground plane	Lg	110
Main patch length	Lm1	21
Parasitic patch length	Lm2	17.95
Lower/upper air height	hm1, hm2	3, 2
Slot major axis length	Lsl1	16.5
Vertical slot width	Lsl2	3.2
Stub length	Lst	2.35
1st binomial section length	Lbt1	11.55
2nd binomial section length	Lbt2	11.82
Branch separation	Ld	6.91
Rectangular stub length/width	Lrs1, Lrs2	3.1, 4
FR4 height	h	1.6
Overall antenna height		3+2+(3×1.6) = 9.8

2.2. Working principles

Radiation from the patches occurs by coupling the electromagnetic energy to patches through elliptic-H slots excited by feed network. The heights of the patch layers are of critical importance for matching, BW, isolation and FBR. Although main patch layer (hm1) has dominant effect in overall design, parasitic patch layer (hm2) must also be considered in combination with it to reach desired technical specifications. The lower hm1 makes efficient coupling from slots to patch easier, hence resulting in good FBR, however this lower hm1 makes broadband operation difficult. The higher hm1 facilitates making antenna broadband but efficient coupling from slots to patch becomes more difficult, hence resulting in poor FBR. Therefore main patch layer must be placed at an optimum height (hm1) together with taking into account its interaction with parasitic patch layer (hm2). At first glance, existence of parasitic patch layer may be questioned because it increases overall antenna profile. However that is not the case because desired technical specifications cannot be attained with a single main patch. In this work, the principal idea is to place main patch at the lowest possible height to have good FBR, and at the same with the proper combination of patches, to reach desired impedance BW, matching level, isolation while also keeping antenna low profile, as it will be more clear in Section 3.

In this study, contrary to conventional rectangular-H slots, center of the slots are redesigned in elliptic form. As addressed in [27], elliptic slot is a simple technique for broadband power transfer between microstrip transitions and employed here as coupled-feeding mechanism. Axial ratio of the ellipse, specifically length of its major axis, controls the level of the coupling. Tapered line nature of elliptic-H slots supports more number of modes to excite patches and hence provide appreciable improvement in impedance BW, matching level and isolation.

Figure 2 plots surface current distributions on the main and parasitic patches at 3.30 GHz and 3.80 GHz as the antenna is excited at port-1. As can be seen in Figure 2a, current amplitude on the main patch gradually increases towards edges at 3.30 GHz in symmetry with $+45^\circ$ diagonal line while the currents are weaker on the parasitic patch. At 3.80 GHz, stronger coupling occurs between two patches and current amplitude on the parasitic patch increases while the main patch has more uniform distribution. This phenomenon indicates the

3. Numerical studies

3.1. Parametric analysis

Proposed antenna is modeled and simulated in Ansoft HFSS. Its electrical performances are numerically analyzed in terms of impedance matching ($|S_{11}|$) and isolation ($|S_{21}|$) with parametric studies. Each parametric study is carried out by sweeping one parameter within a range while the rest is kept unchanged. Since the dual-polarization is obtained using symmetric feeding lines, only $|S_{11}|$ results are reported at Port-1. Upper and lower boundaries of the band of interest (3.30 - 3.80 GHz) are shown with vertical black dashed lines in the figures.

$|S_{11}|$ and $|S_{21}|$ characteristics of proposed antenna as a function of the main patch height (hm1) are given in Figure 3. In this parametric analysis, hm1 is swept in 2–4 mm range by 1 mm steps. Despite the fact that antenna covers larger BW when hm1 = 2 mm, stronger isolation and better matching level with sufficiently large BW are obtained at hm1 = 3 mm. The same procedure is also carried out for the parasitic patch layer height (hm2) and the best performance is achieved when hm2 = 2 mm as shown in Figure 4. With these values (hm1 = 3 mm, hm2 = 2 mm), effect of parasitic patch can be seen better in Figure 5a that desired matching level and impedance BW cannot be achieved with a single main patch. Figure 5b shows simulations of antenna radiation patterns in H-plane plane ($\theta = 90°$, $-180° < \phi < 180°$) by changing hm1 with fixed hm2 = 2 mm. It is observed that FBR gets better at lower hm1 values. As a result, principal design idea to place main patch at the lowest possible height to have good FBR and utilize parasitic patch to reach desired matching level, impedance BW and isolation is consistent. Moreover, overall antenna height can still be kept low profile without using any reflector.

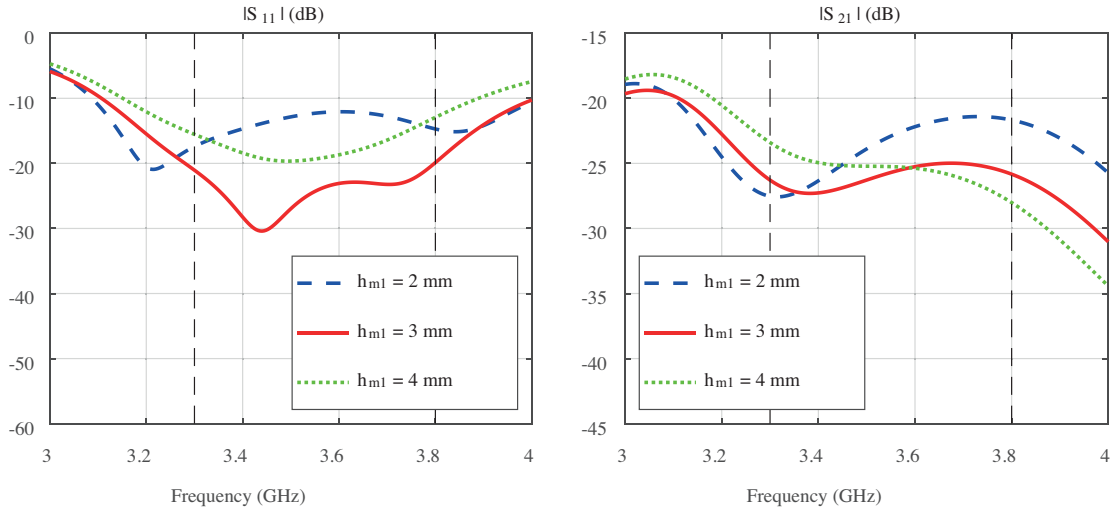


Figure 3. $|S_{11}|$ and $|S_{21}|$ as a function of the main patch height.

Figure 6 illustrates $|S_{11}|$ and $|S_{21}|$ of the antenna regarding axial ratio of the elliptic-H slots, Ax. This analysis is carried out as Ax is increased from 14.5 to 18.5 with increment of 1. When Ax = 16.5, antenna has two resonance points at 3.39 GHz and 3.74 GHz and 20% impedance BW for $|S_{11}| < -15$ dB. Furthermore, the highest isolation is attained at this value of Ax. However, isolation does not vary much with respect to Ax in desired operating band and its typical value is maintained to be $|S_{21}| < -26$ dB.

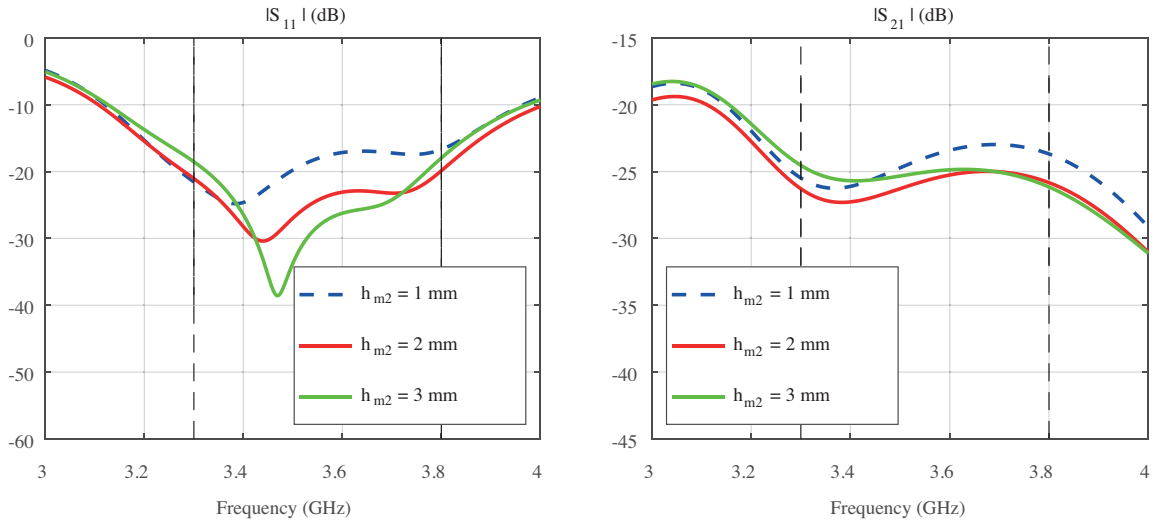


Figure 4. $|S_{11}|$ and $|S_{21}|$ as a function of the parasitic patch height.

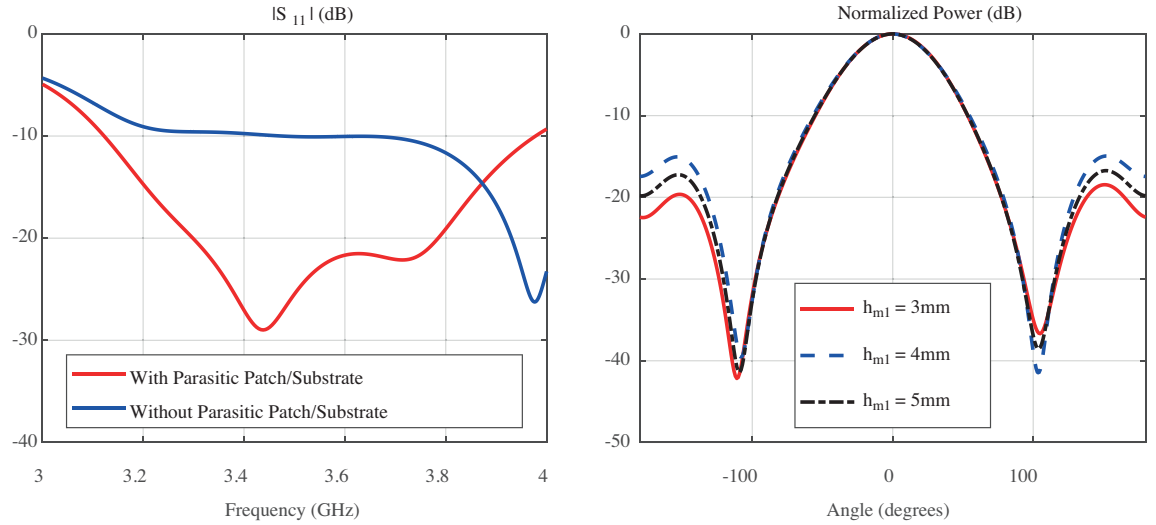


Figure 5. $|S_{11}|$ and $|S_{21}|$ as a function of the parasitic patch height (left). H-plane as function of the main patch height (right).

3.2. Effect of elliptic-H slot

Contribution of elliptic-H slots on the antenna performance is evaluated by comparing it with rectangular-H slots having the same length (Ls = 15.98 mm) and area (Ax $\approx$ 11.186 mm^2). Results of this comparison is illustrated in Figures 7 and 8. It is observed in Figure 7 that elliptic-H slots improve matching level and impedance BW with respect to rectangular-H slots. Improvement in matching level means more efficient energy coupling from slots to patches. The isolation is also improved in the desired band approximately by 3.5 dB with elliptic-H slots.

The mechanism for the isolation improvement can be demonstrated by examining the currents on the slot plane of feedline layer at 3.55 GHz. As shown in Figure 8, the current distribution between the elliptic-H

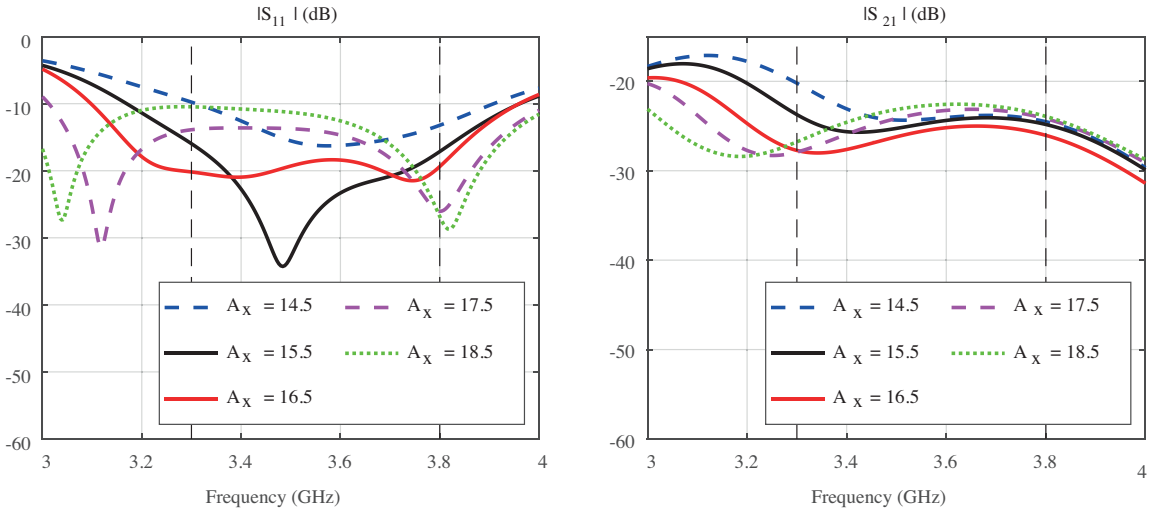


Figure 6. Effect of Ax of elliptic-H slots on $|S_{11}|$ and $|S_{21}|$.

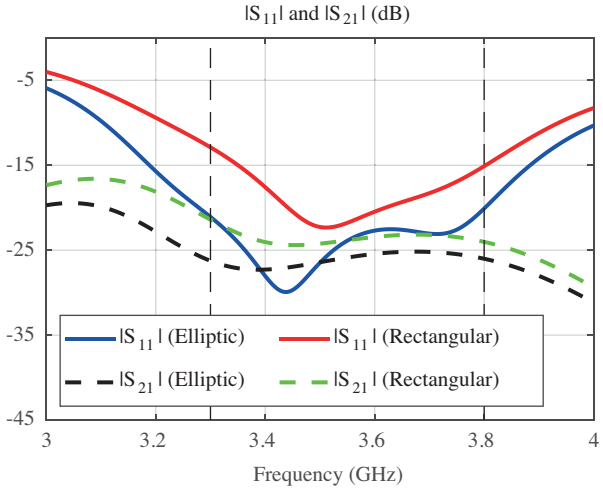


Figure 7. Comparison of elliptic-H slots and rectangular-H slots.

slots, especially around the center where most mutual coupling occurs between ports, are weaker than that of the rectangular-H slots. This weaker flowing current results in improvement in the isolation. As a result, one can say that use of elliptic-H slots helps to have desired matching level, impedance BW, and isolation.

4. Antenna performance

Proposed antenna is prototyped in accordance with descriptions in Section 2 and is shown in Figure 9. Air layers are formed by using plastic separators with appropriate heights. Overall size of the prototype is 110 $mm\times$ 110 $mm\times$ 9.8 mm. The numerical results are experimentally verified by S-parameters ($|S_{11}|$, $|S_{22}|$, and $|S_{21}|$) and radiation patterns (copol, crosspol) measurements. S-parameters are measured by HP 8720D vector network analyzer and radiation pattern measurements are performed in an anechoic chamber that is controlled by a MATLAB-based graphical user interface. The antenna is mounted on an absorptive structure in order to

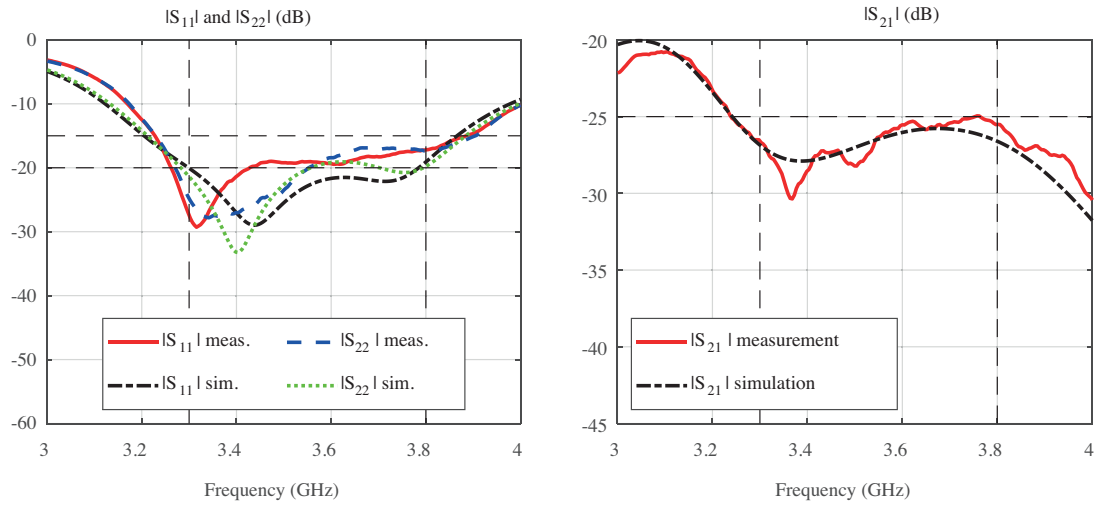


Figure 10. Measured and simulated S-parameters of the prototype.

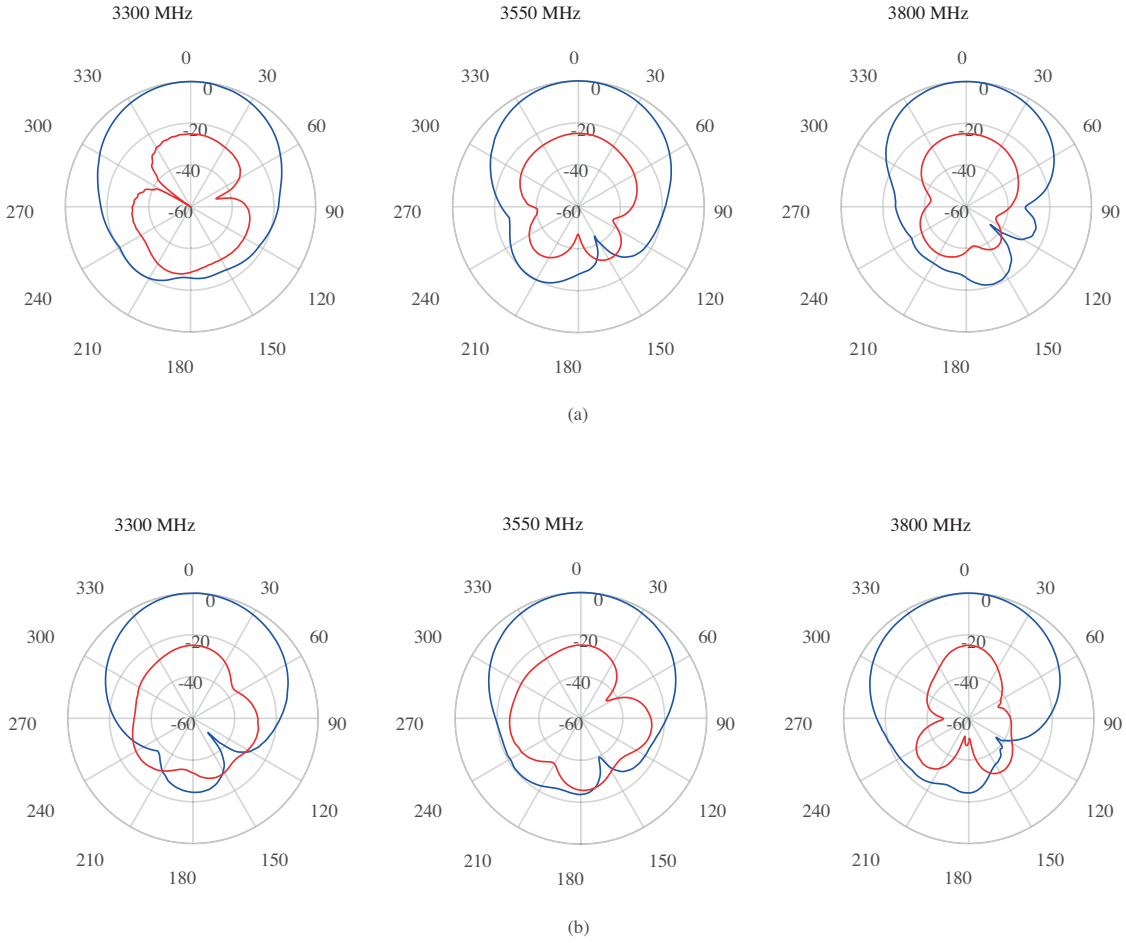


Figure 11. Measured co/crosspol patterns in (a) E-plane and (b) H-plane.

5. Conclusion

Throughout this paper, dual-polarized, broadband, slot-coupled patch antenna in a simple configuration is designed and investigated for sub-6 GHz 5G base stations. Desired operating band is 3.3–3.8 GHz. Proposed antenna is made up of main patch and parasitic patch layers above feedline layer and is excited by crossed elliptic-H slots. In summary, antenna exhibits 18.5% (3.23–3.85 GHz) impedance BW for $|S_{11}|$, $|S_{22}| < -15$ dB, isolation $|S_{21}| < -25$ dB. Antenna also has stable radiation patterns with HPBWs of 59°–64° and 69°–72° in E/H-planes, respectively with gain of 7.9–8.4 dBi. XPD level and FBR are $>$ 22 dB and $>$ 23 dB, respectively.

Simulated and measured radiation patterns show that proposed antenna is low profile with good FBR. As mentioned earlier, slot coupled antennas, in general, have poor FBR performance due to back radiation of slot. And in order to improve FBR, additional reflector plane or cavity backed structure is employed at the expense of increasing the antenna profile. In this design, placement of the main patch at a reasonably low height, then use of parasitic patch in combination with it, and use of elliptic-H slot all together provide the solution and helps to reach design specifications for impedance BW, matching level, isolation and good FBR. The overall height (9.8 mm) of the proposed antenna is still low profile as it can be verified among similar works in Table 2.

Table 2 lists the performances of proposed work and some other similar existing works, which are designed to operate in the same band (3.3–3.8 GHz). In order to make full comparison, note that [5, 6] are crossed-dipole antennas whereas [8] is magneto-electric dipole. [12, 16] are patch antennas with capacitively coupled probe feeds while [19] and [21–24] are slot coupled patch antennas. As can be seen from Table 2, proposed antenna outperforms the cited research by satisfying all the requirements of base station antenna. Considering the numerical and experimental results, proposed dual polarized single element antenna can be a good candidate to be used in the massive MIMO arrays of 5G base stations.

Table 2. Comparison of the related work.

Ref.	**Antenna type**	**BW (GHz, %)**	$\|S_{21}\|$ **[dB]**	**FBR [dB]**	**Height [mm]**	**Refl.**[1]
[5]	Crossed-dipole	3.20–3.90, 19.7% <-15 dB	<-40	>31	14	N/A [2]
[6]	Crossed-dipole	3.50–5.10, 37.2%, <-15 dB	<-20	>10	17	N/A
[8]	Magneto-electric dipole	3.05–4.55, 36.6%, <-15 dB	<-17	>20	21	N/A
[12]	Probe-fed patch	3.15–4.55, 37%, <-10 dB	<-38	>12.5	12.7	N/A
[16]	Probe-fed patch	2.86–4.12, 36%, <-15 dB	<-30	>28	13.4	N/A
[19]	Slot-coupled patch	3.30–3.80, 14%, <-10 dB	<-20	>30	37.2	W [3]
[21]	Slot-coupled patch	3.33–3.83, 14%, <-10 dB	<-23	>25	34	W
[22]	Slot-coupled patch	3.23–3.80, 17%, <-10 dB	<-50	>10	10.5	W/O [4]
[23]	Slot-coupled patch	3.25–3.80, 15.6%, <-15 dB	<-25	>18	12.2	W
[24]	Slot-coupled patch	3.30–3.60, 8.9%, <-15 dB	<-25	>16	18.8	W
This work	Slot-coupled patch	3.20-3.85, 18.5%, <-15 dB	<-25	>23	9.8	W/O

[1]Refl: Reflector.
[2]N/A: Not applicable.
[3]W: With reflector.
[4]W: Without reflector.

Acknowledgment

This work is partially funded by the Scientific and Technological Research Council of Turkey (TÜBİTAK) under grant no. 3180114.

References

[1] Mishra PK, Janagirda DR,Kumar G. A review of broadband dual linearly polarized microstrip antenna designs with high isolation. IEEE Antennas and Propagation Magazine 2014; 56 (6): 238–251. doi: 10.1109/MAP.2014.7011064

[2] Luo Y, Chu QX, Wen DL. A plus/minus 45° dual-polarized base-station antenna with enhanced cross-polarization discrimination via addition of four parasitic elements placed in a square contour. IEEE Transactions on Antennas and Propagation 2016; 64 (4): 1514–1519. doi: 10.1109/TAP.2016.2522463

[3] Ta SX, Park I, Ziolkowski RW. Crossed dipole antennas: A review. IEEE Antennas and Propagation Magazine 2015; 57 (5): 107-122. doi: 10.1109/MAP.2015.2470680

[4] Ding C, Sun H, Ziolkowski RW, Guo YJ. Simplified tightly-coupled cross-dipole arrangement for base station applications. IEEE Access 2017; 5: 27491–27503. doi: 10.1109/ACCESS.2017.2778229

[5] Li M, Chen X, Zhang A, Kishk AA. Dual-polarized broadband base station antenna backed with dielectric cavity for 5G communications. IEEE Antennas and Wireless Propagation Letters 2019; 18 (10): 2051–2055. doi: 10.1109/LAWP.2019 .2937201

[6] Li Y, Wang C, Yuan H, Liu N, Zaho H et al. A 5G MIMO antenna manufactured by 3-D printing method. IEEE Antennas and Wireless Propagation Letters 2017; 16: 657–660. doi: 10.1109/ LAWP.2016.2596297

[7] Hua Q, Huang Y, Alieldin A, Song C, Jia T et al. A Dual-band dual-polarized base station antenna using a novel feeding structure for 5G communication. IEEE Access 2020; 8: 63710-63710. doi: 10.1109/ACCESS.2020.2984199

[8] Sun JN, Li JL, Xia L. A dual-polarized magneto-electric dipole antenna for application to N77/N78 band. IEEE Access 2019; 7: 161708–161715. doi: 10.1109/ACCESS.2019.2951414

[9] Siu L, Wong H, Luk KM. A dual-polarized magneto-electric dipole with dielectric loading. IEEE Transactions on Antennas and Propagation 2009; 57 (3): 616–623. doi: 10.1109/TAP.2009.2013430

[10] Feng B, Zhu C, Cheng JC, Sim CYD, Wen X. A dual-wideband dual-polarized magneto-electric dipole antenna with dual wide beamwidths for 5G MIMO microcell applications. IEEE Access 2019; 7: 43346-43355. doi: 10.1109/ACCESS.2019.2906882

[11] Lai HW, Luk KM. Dual polarized patch antenna fed by meandering probes. IEEE Transactions on Antennas and Propagation 2007; 55 (9): 2625–2627. doi: 10.1109/TAP.2007.904158

[12] Ryu KS, Kishk AA. Wideband dual-polarized microstrip patch excited by hook shaped probes. IEEE Transactions on Antennas and Propagation 2008; 56 (12): 3645–3649. doi: 10.1109/TAP.2008.2007377

[13] Xie JJ, Yin YZ, Wang JH, Liu XL. Wideband dual-polarised electromagnetic fed patch antenna with high isolation and low cross-polarisation. IET Electronics Letters 2013; 49 (3). doi: 10.1049/el.2012.3934

[14] Jin Y, Du Z. Broadband dual-polarized F-probe fed stacked patch antenna for base stations. IEEE Antennas and Wireless Propagation Letters 2015; 14: 1121-1124. doi: 10.1109/LAWP.2015.2395422.

[15] Mak KM, Lai HW, Luk KM. A 5G wideband patch antenna with antisymmetric L-shaped probe feeds. IEEE Transactions on Antennas and Propagation 2018; 66 (2): 957-961. doi: 10.1109/TAP.2017.2776973

[16] Ciydem M, Miran EA. Dual polarization wideband sub-6 GHz suspended patch antenna for 5G base stations. IEEE Antennas and Wireless and Propagation Letters 2020; 19 (7): 1142-1146. doi: 10.1109/ LAWP.2020.2991967

[17] Barba M. A high-isolation, wideband and dual-linear polarization patch antenna. IEEE Transactions on Antennas and Propagation 2008; 56 (5) 1472–1476. doi: 10.1109/TAP.2008.922889

[18] Serra AA, Nepa P, Manara G, Tribellini G, Cioci S. A wideband dual-polarized stacked patch antenna. IEEE Antennas and Wireless Propagation Letters 2007; 6: 141–143. doi: 10.1109/LAWP.2007.893101

[19] Wong KL, Tung HC, Chiou TW. Broadband dual-polarized aperture-coupled patch antennas with modified H-shaped coupling slots. IEEE Transactions on Antennas and Propagation 2002; 50 (2): 188–191. doi:10.1109/8.997993

[20] Kirov GS, Mihaylova DP. Circularly polarized aperture coupled microstrip antenna with resonant slots and a screen. Radioengineering 2010; 19 (1): 111–116.

[21] Caso R, Serra A, Buffi A, Rodriguez-Pino M, Nepa P. Dual-polarized slot-coupled patch antenna excited by a square ring slot. IET Microwaves Antennas and Propagation 2011; 5 (5): 605–610. doi: 10.1049/IET-MAP.2010.0460

[22] Hua C, Li R, Wang Y, Lu Y. Dual-polarized filtering antenna with printed Jerusalem-cross radiator. IEEE Access 2018; 6: 9000–9005. doi: 10.1109/ACCESS.2018.2803790

[23] Lu J, Kuai Z, Zhu X, Zhang N. A high-isolation dual-polarization microstrip patch antenna with quasi-cross-shaped coupling slot. IEEE Transactions on Antennas and Propagation 2011; 59 (7): 2713–2717. doi: 10.1109/TAP.2011.2152333

[24] Alieldin A, Huang Y, Stanley M, Joseph SD, Lei D. 5G MIMO antenna for broadcast and traffic communication topologies based on pseudo inverse synthesis. IEEE Access 2018; 6: 65935–65945. doi: 10.1109/ACCESS.2018.2878639

[25] Huang H, Li X, Liu Y. 5G MIMO antenna based on vector synthetic mechanism. IEEE Antennas and Wireless Propagation Letters 2018; 17 (6): 1052–1055. doi: 10.1109/LAWP.2018.2830807

[26] Liu Y, Wang S, Wang X, Jia Y. A differentially fed dual-polarized slot antenna with high isolation and low profile for base station application. IEEE Antennas and Wireless Propagation Letters 2019; 18 (2): 303-307. doi: 10.1109/LAWP.2018.2889645

[27] Abbosh AM. Ultra-wideband vertical microstrip-microstrip transition. IET Microwaves Antennas and Propagation 2007; 1 (5): 968–972. doi: 10.1049/IET-MAP:20070043